




Technical Note

Examples of Application of ^{GA}SAKe for Predicting the Occurrence of Rainfall-Induced Landslides in Southern Italy

Oreste Terranova ¹ , Stefano Luigi Gariano ^{2,*} , Pasquale Iaquinta ¹, Valeria Lupiano ¹, Valeria Rago ¹ and Giulio Iovine ¹ 

¹ Istituto di Ricerca per la Protezione Idrogeologica (IRPI), Consiglio Nazionale delle Ricerche (CNR), via Cavour 6, 87036 Rende (CS), Italy; oreste.terranova@irpi.cnr.it (O.T.); pasquale.iaquinta@irpi.cnr.it (P.I.); valeria.lupiano@irpi.cnr.it (V.L.); valeria.rago@irpi.cnr.it (V.R.); giulio.iovine@irpi.cnr.it (G.I.)

² Istituto di Ricerca per la Protezione Idrogeologica (IRPI), Consiglio Nazionale delle Ricerche (CNR), via Madonna Alta 126, 06128 Perugia, Italy

* Correspondence: gariano@irpi.cnr.it; Tel.: +39-075-5014-424

Received: 12 January 2018; Accepted: 22 February 2018; Published: 24 February 2018

Abstract: ^{GA}SAKe is an empirical-hydrological model aimed at forecasting the time of occurrence of landslides. Activations can be predicted of either single landslides or sets of slope movements of the same type in a homogeneous environment. The model requires a rainfall series and a set of dates of landslide activation as input data. Calibration is performed through genetic algorithms, and allows for determining a family of optimal kernels to weight antecedent rainfall properly. As output, the mobility function highlights critical conditions of slope stability. Based on suitable calibration and validation samples of activation dates, the model represents a useful tool to be integrated in early-warning systems for geo-hydrological risk mitigation purposes. In the present paper, examples of application to three rock slides in Calabria and to cases of soil slips in Campania are discussed. Calibration and validation are discussed, based on independent datasets. Obtained results are either excellent for two of the Calabrian rock slides or just promising for the remaining case studies. The best performances of the model take advantage of an accurate knowledge of the activation history of the landslides, and a proper hydrological characterization of the sites. For such cases, ^{GA}SAKe could be usefully employed within early-warning systems for geo-hydrological risk mitigation and Civil Protection purposes. Finally, a new release of the model is presently under test: its innovative features are briefly presented.

Keywords: landslide forecasting; threshold; hydrological model; genetic algorithms; Calabria; Campania

1. Introduction

Rainfall-induced landslides often cause significant economic loss and casualties in Calabria, as in most part of the Italian Peninsula [1,2]. Therefore, their prediction assumes a crucial role in geo-hydrological risk mitigation. The timing of activation of such phenomena is usually predicted by means of either empirical (e.g., [3] and references therein) or physically-based [4–6] approaches. To relate rainfall to time of slope instability, the extent of the landslide and the physical characteristics of both rainfall and involved materials (soil/rock) must be considered—e.g., in terms of intensity, duration, amount, and of infiltration capacity. Unfortunately, because of the high cost of field investigations, the parameters required by the physically-based approach are known only for a very limited number of case studies. Therefore, to model the triggering conditions of slope movements—either shallow or deep-seated—a threshold-based modelling approach can be employed [7,8]. Empirical thresholds can be expressed in terms of curves, delimiting the portion

of Cartesian planes containing rainfall or hydrological conditions related to known activations. Examples of definition and application of empirical rainfall thresholds in Southern Italy are provided by [9–13]. In hydrological models, kernels (or filter functions) are commonly employed to express the influence of rainfall on runoff and groundwater dynamics: they are usually defined in terms of a simple, continuous analytical function. The base time (t_b) of a given kernel expresses the temporal extent in which rainfall seems to have a significant effect on slope stability. The shape and the base time of the kernel are related to magnitude of the landslide and to hydro-geological complexity of the site under investigation. Finally, the predictive tool (named mobility function) can be obtained through the convolution integral between the kernel and the rainfall series [14–16].

2. Materials and Methods

$^{GA}SAKe$ (Genetic-Algorithm-based Self Adaptive Kernel) is an empirical-hydrological model for predicting the timing of activation of slope movements of different types [17]. A linear and steady slope-stability response to rainfall and a classic threshold scheme are assumed in the model: the exceedance of the threshold determines the triggering of the landslide [18]. Though inspired by the *FLaIR* (Forecasting Landslides Induced by Rainfall) model [19,20] (already applied in several case studies, see [21–23]), it differs for several features and is suitable to handle complex cases: in fact, the model adopts a discrete kernel, instead of a continuous one, and is based on a genetic-algorithm procedure that allows for an effective, automated, self-adaptive calibration. The model can be applied either to single landslides, characterized by several historical activations, or to a set of similar slope movements in a homogeneous geomorphological context. Case studies may be of any depth, from shallow to deep-seated. The inputs of the model are: (i) the rainfall series and (ii) the set of known dates of landslide activation. Regarding rainfall data, $^{GA}SAKe$ needs as input a single rainfall series at a given time scale (e.g., daily, hourly, sub-hourly rainfall); the series can be derived from one only rain gauge or by combining rainfall data from different gauges into a “synthetic” series (e.g., by means of geostatistical techniques). The temporal extent of the rainfall series must start before the first landslide activation date and terminate after the last date (e.g., at the beginning and at the end of hydrological years). The mobility function—i.e., the output of the model as obtained through calibration—highlights the most critical conditions for the stability of the considered case study: its values depend on both rainfall amounts and shape/base time of the kernel. Triggering conditions occur when the value of the mobility function exceeds a given threshold.

More in detail, calibration of the model is based on genetic algorithms (“GA”, in the following; [24,25]), which allow to obtain families of optimal, discretized solutions (kernels) that maximize the fitness function. At the beginning of a given optimization experiment, a family of kernels is randomly generated. The application to such kernels of a sequence of genetic operators—namely *selection*, *crossover* and *mutation*—constrained by prefixed probabilities, allows to generate a new population of candidate solutions (genotypes), to be tested as kernels in the successive GA iteration. A mobility function (phenotype) is then obtained by convolution between each kernel and rainfall, and its performance is evaluated by applying a suitable fitness function. Thanks to inherent properties of GA (cf., Fundamental Theorem [24]), better individuals (i.e., characterized by higher fitness values) can be obtained over time through iterations.

In $^{GA}SAKe$ the evaluation of the phenotypes (and, therefore, of the related genotypes) is primarily based on the *fitness values*, Φ , defined on the relative position (*rank*, k_i) of the peaks of the mobility function corresponding to the L dates of landslide activation [17]. It is:

$$\Phi = \frac{\sum_{i=1}^L k_i^{-1}}{\sum_{i=1}^L i^{-1}}. \quad (1)$$

When two (or more) mobility functions share the same value of fitness, a further distinction can be made based on the safety margin, Δz_{cr} , defined as:

$$\Delta z_{cr} = (z_{j-\min} - z_{cr}) / z_{j-\min}, \tag{2}$$

in which $z_{j-\min}$ is the height of the lowest peak of the mobility function that corresponds to one of the activation dates, and z_{cr} is the critical height, i.e., the height of the highest peak of the mobility function located just below $z_{j-\min}$. Kernels with similar Φ can therefore be distinguished, and those more useful for predictive purposes selected, being characterized by larger separations among the peaks of the mobility function either corresponding to dates of activation or not.

Over several GA iterations, the mobility function is forced toward a shape characterized by peaks coinciding with the dates of landslide occurrence. An optimal kernel leads to a mobility function having the highest peaks in correspondence to such dates; further peaks may also be present, but characterized by lower values.

The best Q kernels obtained in the calibration phase can be utilized to synthesize “average” kernels to be employed for validation, by considering further dates of landslide activation (and appropriate rainfall series). Up to date, a set of Q = 100 optimal kernels has been employed during tests and first applications of the model to several case studies in Southern Italy. Once validated, the model can finally be applied—e.g., in support of an early-warning system—to estimate the timing of future landslide activations in the same study area, by employing measured or forecasted rainfall. In Figure 1, the calibration and validation procedures are schematically shown. For the sake of brevity, a complete description of the model is not reported here; however, a more detailed overview of its main features and of the calibration/validation procedures can be found in [3].

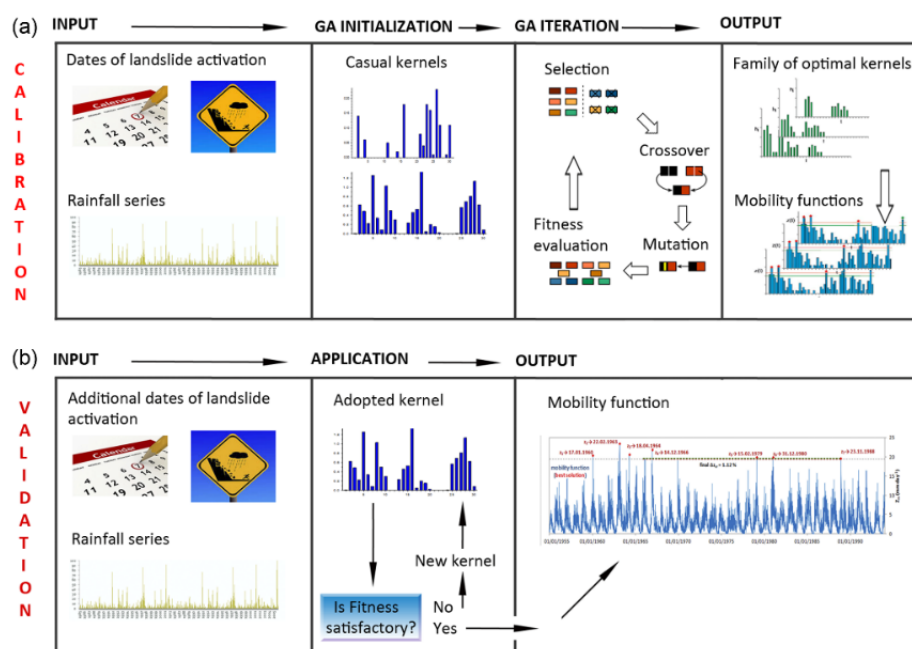


Figure 1. Schematic sketch of: (a) the calibration and (b) the validation procedures of $GAsAKE$.

3. Case Studies

The model was applied to different case studies in Southern Italy (Figure 2), and precisely to 3 rock slides in northern Calabria and to a set of shallow landslides (soil slip-debris flows) in Campania. Table 1 lists the average rainfall recorded near the considered case studies, while Tables 2 and 3 list the main characteristics of the considered slope movements.

Table 1. Average monthly and annual rainfall (MR, in mm) and number of rainy days (MRD) at rain gauges near the considered case studies. Key: (AC) Acri rain gauge (750 m a.s.l.); (MU) Montalto Uffugo rain gauge (468 m a.s.l.); (GR) Gragnano rain gauge (185 m a.s.l.).

Rain Gauge	Variable	September	October	November	December	January	February	March	April	May	June	July	August	Year
AC	MR	57.9	105.7	130.5	160.1	141.4	120.8	102.4	73.6	54.8	24.4	16.2	24.7	1012.4
	MRD	6	9	10	13	13	11	10	9	6	3	2	3	96
MU	MR	70.4	125.1	187.9	220.8	198.1	160.3	132.8	98.9	64.6	27.8	18.3	28.6	1333.6
	MRD	7	11	13	14	14	13	13	11	8	5	3	4	114
GR	MR	90.1	144.8	202.1	209.3	181.1	152.8	119.0	106.4	62.7	31.8	23.2	36.4	1359.7
	MRD	6	9	12	10	11	10	9	9	7	4	3	3	94

Table 2. Main characteristics of the Calabrian case studies. In *Italics*, the dates of activation used for validation. Employed data series range from the beginning of the calibration periods to the end of the validation period (cf. last column). No missing data characterize the considered rain series.

Landslide (Involved Lithotype)	Landslide Type	Dimensions	Activation Dates	Optimization Periods (Rain Gauge, Distance from Landslides)
Acri—Serra di Buda (Palaeozoic metamorphic and intrusive rocks)	rock slide	length: 550 m width: 400 m depth: 45–50 m	(1) 20.11.1937 (2) 29.12.1937 (3) 12.1944–01.1945 (4) 01.12.1980 (5) 28.11.1984 (6) 01.04.1985	calibration period: 01.01.1932–31.01.1985 validation period: 01.02.1985–01.06.1985 (Acri, 1.2 km)
San Benedetto Ullano—San Rocco (Palaeozoic metamorphic rocks)	rock slide	length: 550 m width: 300 m depth: 15–35 m	(1) 28.01.2009 (2) 31.01.2010 (3) 15.03.2013	calibration period: 01.01.1970–30.04.2010 validation period: 01.05.2010–30.04.2013 (Montalto Uffugo, 3.5 km)
San Fili—Uncino (Miocene sedimentary rocks overlying Palaeozoic metamorphic rocks)	rock slide	length: 650 m width: 200 m depth: 25–30 m	(1) 16.01.1960 (2) 01.11.1962–14.04.1963 (3) 15.04.1964 (4) 14.12.1966 (5) 13.02.1979 (6) 12.1980	calibration period: 01.09.1959–31.08.1980 validation period: 01.09.1980–31.03.1981 (Montalto Uffugo, 8 km)

Table 3. Main characteristics of the considered Campanian case studies. Key: (M) multiple activation; (S) single activation. In Italics, the date of activation used for validation. Employed data series range from the beginning of the calibration periods to the end of the validation period (cf. last column). The Gragnano rain gauge was employed for the Campanian cases. Missing values (about 2% of the whole set) were taken from the Castellammare and Tramonti-Chiunzi gauges.

Landslide (Involved Lithotype)	Landslide Type	Average Dimensions	Activation Dates (Type)/Affected Site	Optimization Periods (Rain Gauge, Average Distance from Landslides)
Sorrento Peninsula (Pleistocene volcanic and volcanoclastic deposits overlaying Mesozoic limestone)	soil slip	source area: 100–20000 m ² source depth: 0.5–4 m	(1) 17.02.1963 (M)/Gragnano, Pimonte, Castellammare. (2) 23.11.1966 (S)/Vico Equense (Scrajo), Arola, Ticciano. (3) 15–24.03.1969 (M)/Cava de' Tirreni, Agerola, Scrajo Seiano. (4) 02.01.1971 (S)/Gragnano. (5) 21.01.1971 (S)/Gragnano. (6) 04.11.1980 (S)/Vico Equense (Scrajo). (7) 14.11.1982 (S)/Pozzano. (8) 22.02.1986 (M)/Palma Campania, Castellammare, Vico Equense. (9) 23.02.1987 (S)/Gragnano, Castellammare. (10) 23.11.1991 (S)/Pozzano. (11) 10.01.1997 (M)/Pozzano, Castellammare, Nocera, Pagani, <i>Amalfitana Coast.</i>	calibration: 17.01.1963–10.12.1996 validation: 11.12.1996–10.02.1997 (Gragnano, Castellammare, and Tramonti-Chiunzi, 4.5 km)

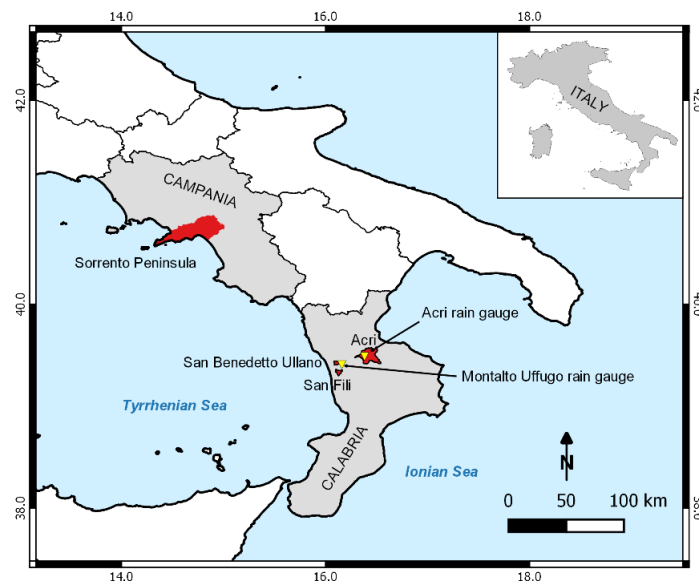


Figure 2. Location of the case studies (marked in red) in Calabria and Campania regions (marked in grey). Yellow triangles indicate Aciri and Montalto Uffugo rain gauges.

3.1. Calabrian Case Studies

Calabria is an accretionary wedge made of a series of Jurassic to Early Cretaceous ophiolite-bearing tectonic units, plus overlying Hercynian and pre-Hercynian basement nappes [26]. Because of its geodynamic history [27–30], the lithological units that make up the Calabrian Arc are commonly characterized by pervasive fracture systems that favored the development of severe weathering processes. The combined effect of tectonic disturbance, differentiated uplift, erosive processes, and chemical-physical alteration influenced physiographic setting of the region, allowing for widespread slope movements of various types and extensions. In addition to earthquakes, meteoric events represent the main triggering factor of landslides in Calabria [31]. These latter pose serious risk conditions in much of the region [32–39]. The climate is Mediterranean (Csa, according to [40]). The Tyrrhenian sector is rainier than the Ionian one (1200–2000 mm vs. 500 mm); nevertheless, the most severe storms occur more frequently on the Ionian side of the region [41]. According to [42], heavy and frequent winter rainfall, caused by cold fronts mainly approaching from NW, and autumn rains, determined by cold air masses from NE, affect the region. In spring, rains show lower intensities than in autumn, while strong convective storms are common at the end of summer. Average yearly rainfall varies between 1000 and 2000 mm/y in mountainous and internal areas, and between 600 and 900 mm/y in coastal areas, with a mean regional value of about 1150 mm/y. Over 70% of the yearly precipitation occurs from October to March, with negligible monthly values from June to September. Concerning the effects of climate change in Calabria, a reduction of annual and winter amounts and an increase of summer rainfall has been recorded in the past decades (e.g., [43,44]).

3.1.1. The Aciri—Serra di Buda Landslide

The village of Aciri (Figure 3) is located on the Sila Massif, on the right flank of the Crati Graben, a tectonic depression belonging to the Calabrian-Sicilian Rift Zone [27]. The area is marked by a couple of regional, recent/active systems, made of N–S trending normal faults and of WNW–ESE trending strike-slip faults [45,46]. Along the N–S trending system, Palaeozoic metamorphic and igneous rocks (gneiss and granite, commonly weathered) of the Sila Massif, to the East, give place to Late Miocene-Quaternary sediments (mainly conglomerate, sand and clay) of the graben, to the West [47].

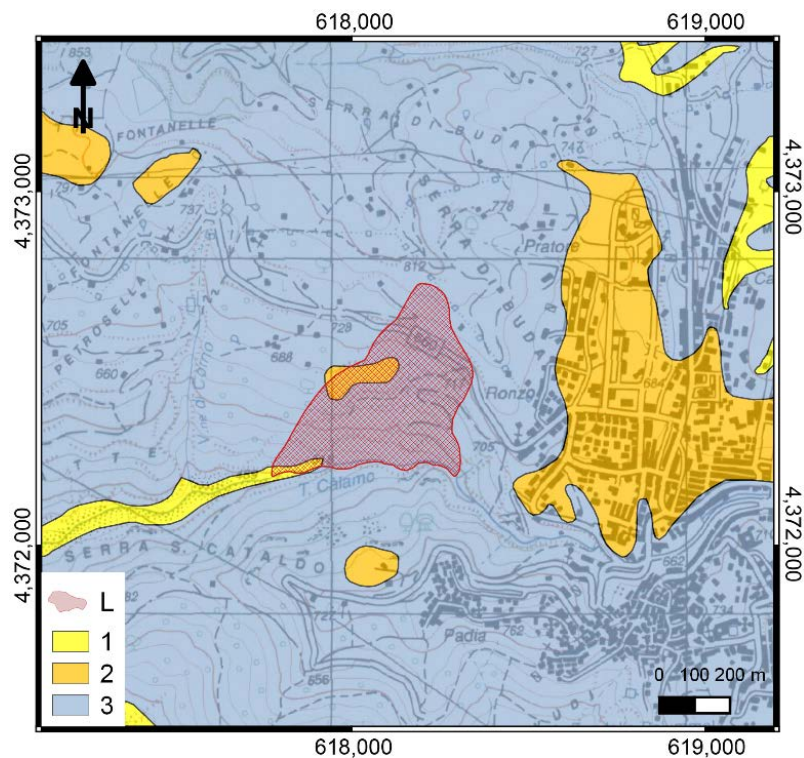


Figure 3. Lithological sketch of the Serra di Buda landslide at Acri. Key: (1) Alluvium, colluvium and residual soil; (2) conglomerate and sandstone; (3) Igneous and medium-high grade metamorphic rock. The landslide (L) is marked by a red hatched polygon. Topographic base map after 1:25,000 IGMI sheets; lithological map after [47], Geological map of Calabria (scale 1:25,000), mod.

The translational rock slide of Serra di Buda is a portion of a Sackung [48] that threatens the surroundings of the village of Acri. The landslide involves weathered gneissic and granitic rocks. In the last 100 years, it suffered from several reactivations and the Civil Authorities had to close the state road to traffic on several occasions, thus causing serious connection problems with the main urban centers of the area (mainly located in the nearby valley). In the present study, only a subset of the known dates of activation are considered: based on hydrological analyses, [49] showed either scarce or no direct correlation between some of the historical dates of mobilization and rainfall amounts. For such dates, further analyses are needed to better evaluate the possible causes of activation [50].

3.1.2. The San Benedetto Ullano—San Rocco Landslide

The village of San Benedetto Ullano (Figure 4) is located on the left flank of the Crati Graben, at the base of the Coastal Chain. The area is marked by the San Fili-San Marco Argentano normal fault, a N–S trending active structure ca. 30 km long. Along the fault, the metamorphic rocks (mainly gneiss, schist and phyllite) of the Coastal Chain, to the West, give place to Pliocene-Quaternary sediments (conglomerate, sand and clay) and subordinate Miocene outcrops (conglomerate and evaporate rocks), to the East [47]. Note that, at the rain gauge of Montalto Uffugo (in the surroundings of San Benedetto Ullano), the highest Calabrian amounts of mean annual rainfall are recorded.

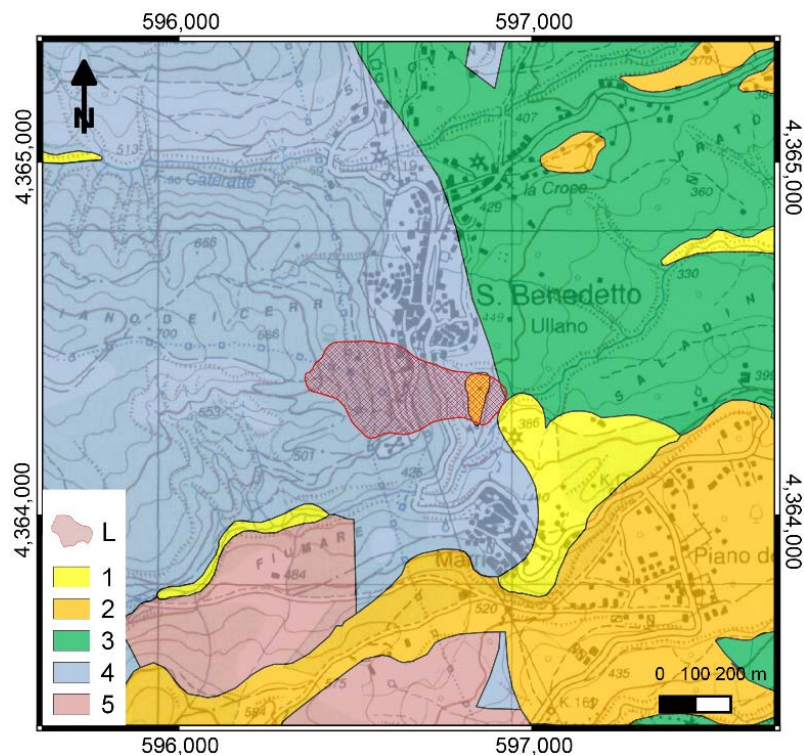


Figure 4. Lithological sketch of the San Rocco landslide at San Benedetto Ulliano. Key: (1) Alluvium, colluvium, and residual soil; (2) conglomerate and sandstone; (3) Clay and clayey flysch; (4) Igneous and medium-high grade metamorphic rock; (5) Argillite and low-grade metamorphic rock. The landslide (L) is marked by a red hatched polygon. Topographic base map after 1:25,000 IGMI sheets; lithological map after [47], Geological map of Calabria (scale 1:25,000), mod.

The San Rocco translational rock slide developed mainly in gneissic rocks at the southern margin of the village, between the historical center and the cemetery [14,51,52]. Between January 2009 and March 2013, a series of 3 major re-activations was observed, with serious damage to the provincial road; the Cemetery and several buildings at the southern margin of the village were also affected by widespread opening of fissures and fractures.

3.1.3. The San Fili—Uncino Landslide

The village of San Fili (Figure 5) is located on the left flank of the Crati graben. In the area, N–S trending normal faults mark the transition between Palaeozoic weathered metamorphic rocks of the Coastal Chain (migmatitic gneiss and biotitic schist), mantled by a late Miocene sedimentary cover of conglomerate, arenite and marly clay, to the West, and Pliocene–Quaternary sediments (sand and clay) of the graben, to the East [47]. The village lies in the intermediate sector between two faults, cut by a NE–SW trending connection fault delimiting Miocene sediments, to the North, from gneissic rocks, to the South.

The Uncino rock slide developed at the western margin of San Fili, involving Miocene sediments (clay and subordinate sandstone) overlaying Palaeozoic metamorphic rocks (gneiss and biotitic schist). In historical time, the slope movements repeatedly affected the village, damaging the railway and the local road network, as well as some buildings: the most ancient known activation dates to the beginning of the twentieth century [53]; from 1960 to 1990, the regional railroad was frequently damaged or even interrupted [54]. Cumulated antecedent rains corresponding to known activations of the Uncino landslide were analyzed by considering the records of the Montalto Uffugo rain gauge [17].

Based on trends of antecedent rains in the 30–180 days before activations, the activation dates to be used for hydrological analyses could be selected.

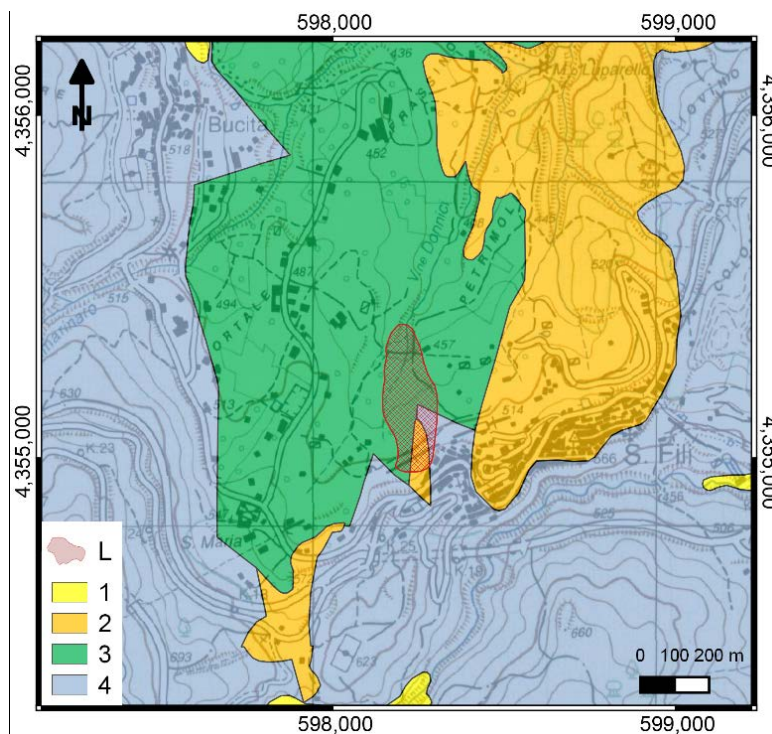


Figure 5. Lithological sketch of the Uncino landslide at San Fili. Key: (1) Alluvium, colluvium, and residual soil; (2) conglomerate and sandstone; (3) Clay and clayey flysch; (4) Igneous and medium-high grade metamorphic rock. The landslide (L) is marked by a red hatched polygon. Topographic base map after 1:25,000 IGMI sheets; lithological map after [47], Geological map of Calabria (scale 1:25,000), mod.

3.2. Campanian Case Studies

The Sorrento Peninsula (Figure 6) is in western Campania, Southern Italy, within the frame of the Neogene Apennine Chain [55]. In the area, Mesozoic limestone mainly crops out, covered by Miocene flysch, Pleistocene volcanic deposits (pyroclastic fall, ignimbrite), and Pleistocene detrital–alluvial deposits [56]. The carbonate bedrock constitutes a monocline, gently dipping towards WNW, mantled by sedimentary and volcanoclastic deposits, with thicknesses ranging from a few decimeters to tens of meters.

Hot, dry summers and moderately cold and rainy winters characterize the study area; its climate is Mediterranean (Csa, according to [40]). Average annual rainfall varies from 900 mm, west of Sorrento, to 1500 mm at Mt. Faito; moving inland to the East, it reaches 1600 mm at Mt. Cerreto and 1700 mm at the Chiunzi pass [57]. On average, annual totals are concentrated on about 95 rainy days. During the driest 6 months (from April to September), only 30% of the annual rainfall is recorded in about 30 rainy days. During the three wettest months (November, October, and December), a similar amount is recorded in about 34 rainy days [58]. In the area, convective rainstorms commonly occur at the beginning of the rainy season (from September to October). In autumn–winter, either high intensity or long duration rainfall are usually recorded, while uniformly distributed rains generally occur in spring. Both at sea level and higher elevations, the southern slopes of the Peninsula are characterized by smaller average annual maxima of daily rainfall with respect to the northern slopes [59]. Severe storms frequently trigger shallow landslides in the volcanoclastic cover of the Peninsula. Landslide sources show a wide range of planforms (i.e., elongated, triangular, grape-like

and compound), extensions (from 100 m up to 20,000 m²), and depths (from 0.5 to 4 m). Soil slips usually propagate seaward as either debris flows or avalanches, often increasing their original volume by entraining material along the tracks, and eventually causing casualties and serious damage to urbanized areas and transportation facilities [60–62].

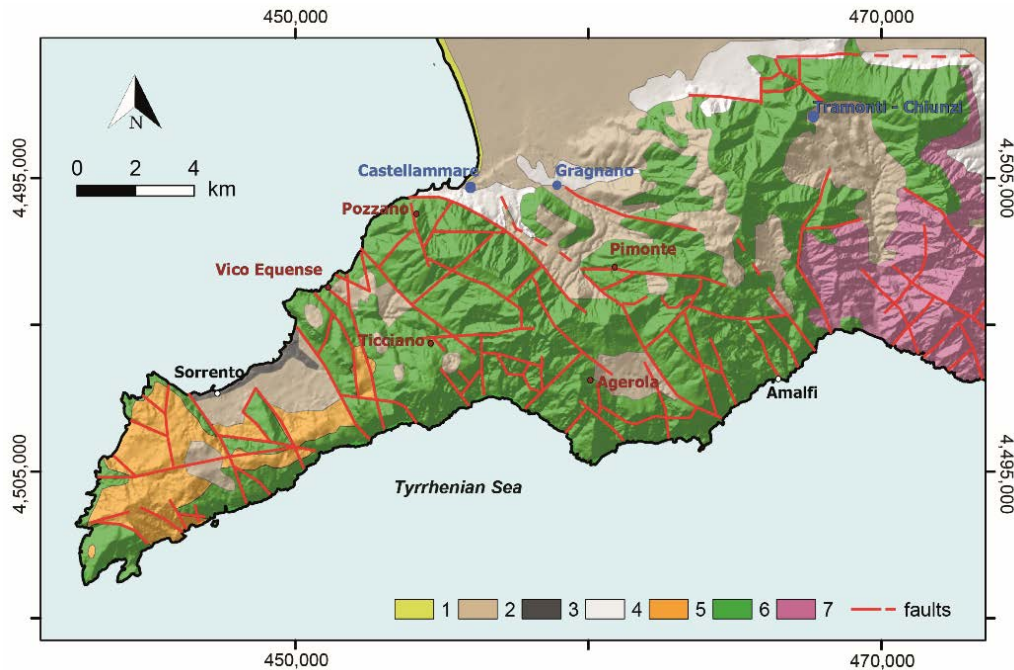


Figure 6. Lithological sketch of the Sorrento Peninsula. Key: (1) beach deposit (Holocene); (2) pyroclastic fall deposit (late Pleistocene–Holocene); (3) Campanian ignimbrite (late Pleistocene); (4) detrital alluvial deposit (Pleistocene); (5) flysch deposit (Miocene); (6) limestone (Mesozoic); (7) dolomitic limestone (Mesozoic). Red lines mark the main faults; red circles and red labels, the sites affected by shallow landslide activations; blue circles, the rain gauges; white circles, the main localities (after [17], mod.).

In the second half of the 20th century, shallow landslides activated on several occasions nearby Castellammare di Stabia: in Table 3, the major events recorded between Vico Equense and Gragnano are listed, with details on types of events and affected sites. All such events occurred between November and March, a period characterized by a medium to low suction range and included in the rainy season (October to April), according to [63]. Rainfall responsible for landslide occurrences in the Sorrento Peninsula were extracted from the records of the nearest gauges (i.e., Gragnano, Castellammare, and Tramonti-Chiunzi; Figure 6). The trends of antecedent rains look quite different. Based on hydrological consideration, the dates of activation were selected for calibration and validation of the model.

4. Results and Discussion

For each case study, the model was optimized by considering a subset of calibration dates, and then validated against further dates of activation. The calibration and validation periods were defined based on rainfall data availability, seasonality, and quality of information on activation dates (Tables 2 and 3). More in detail, optimal kernels were obtained in calibration by averaging the best 100 filter functions. Validation was then performed by applying such average kernels to the remaining activation dates (i.e., a temporal validation was performed). The optimal kernels and mobility functions for the considered case studies are shown in Figures 7–10. Calibration and validation results are synthesized in Table 4.

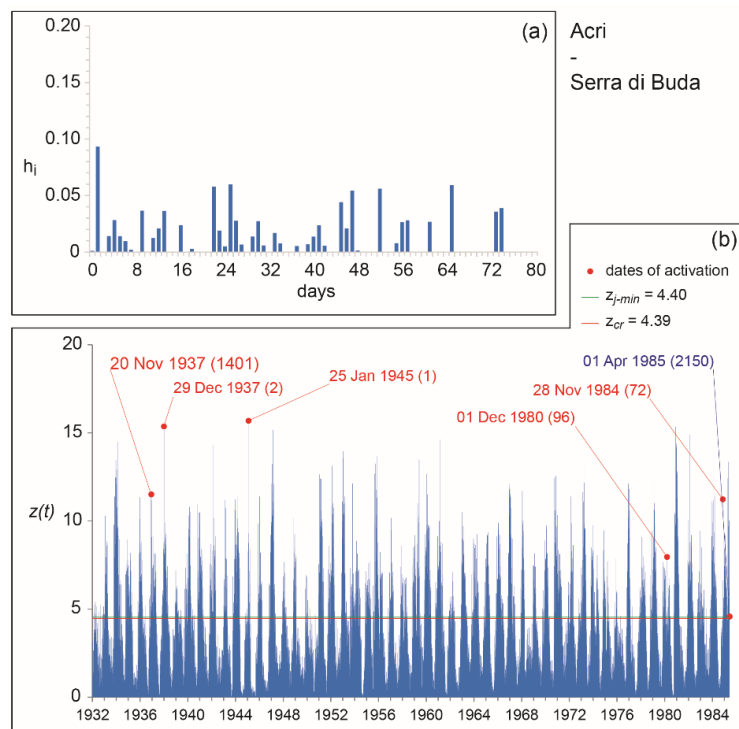


Figure 7. Acri—Serra di Buda case study: (a) optimal kernel; (b) mobility function obtained by applying the optimal kernel to the entire set of available activation dates (cf. [50]).

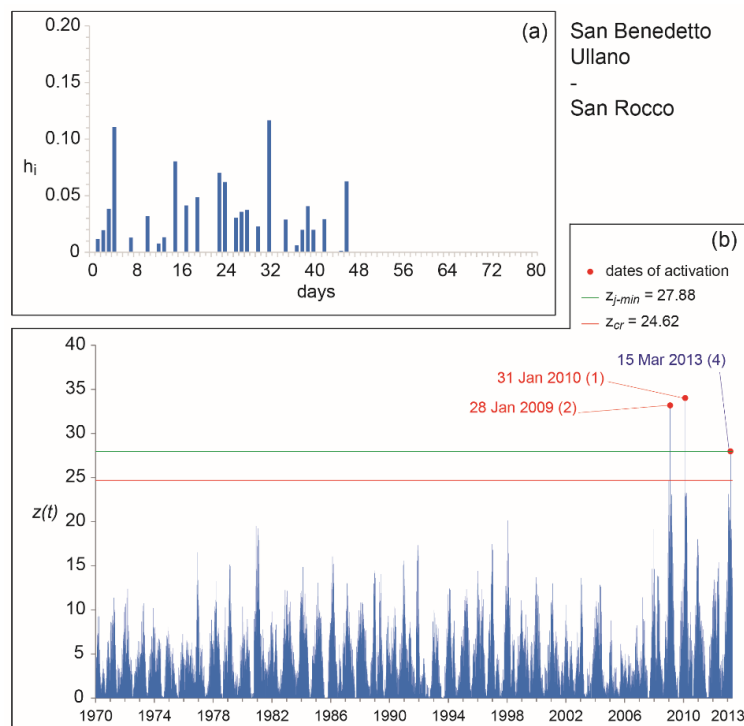


Figure 8. San Benedetto Ullano—San Rocco case study: (a) optimal kernel; (b) mobility function obtained by applying the optimal kernel to the entire set of available activation dates (cf. [54,64]).

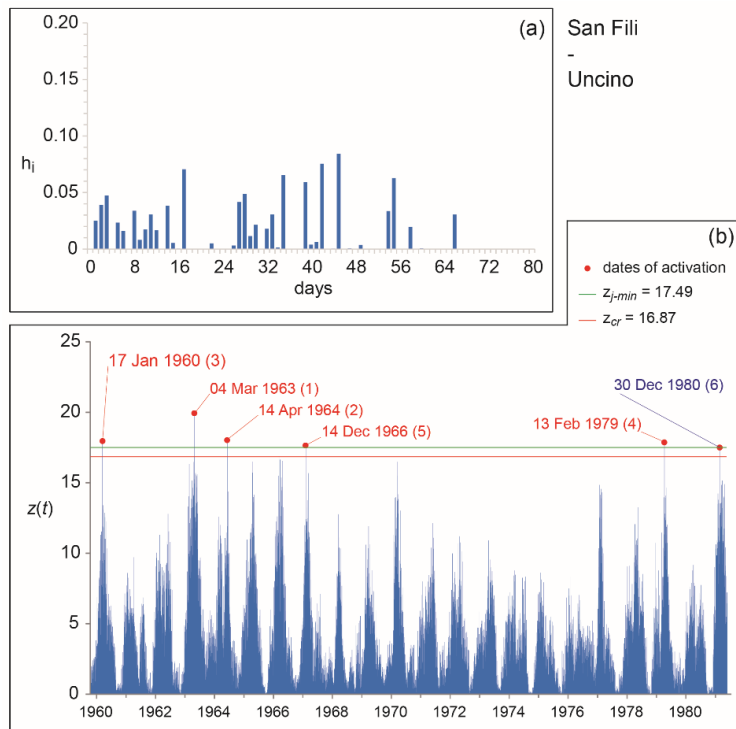


Figure 9. San Fili—Uncino case study: (a) optimal kernel; (b) mobility function obtained by applying the optimal kernel to the entire set of available activation dates (cf. [17]).

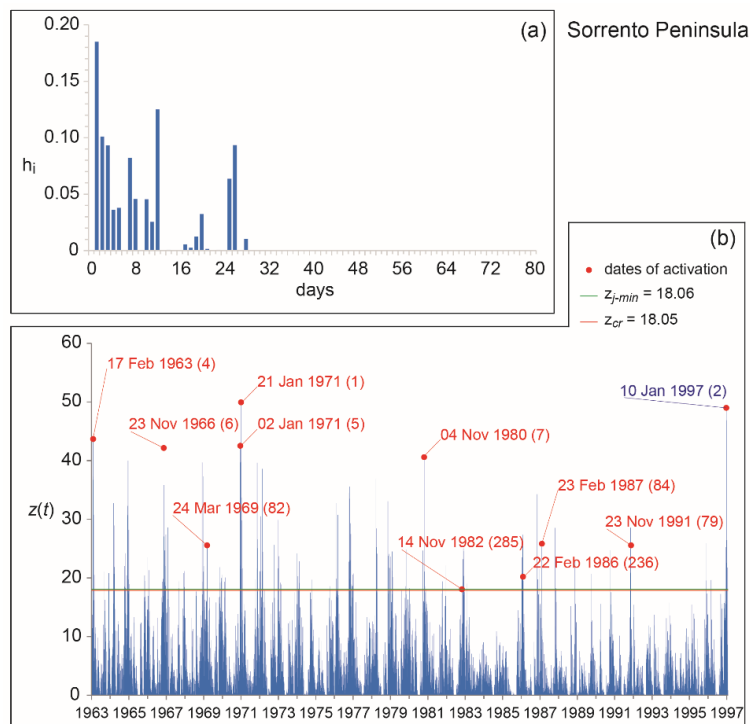


Figure 10. Sorrento Peninsula case study: (a) optimal kernel; (b) mobility function obtained by applying the optimal kernel to the entire set of available activation dates (cf. [17]).

Table 4. Model results for the considered case studies. For each case, the following details are listed: landslide type; number of activation dates employed for calibration and validation; base time of the optimal kernel; maximum fitness obtained in calibration and in validation.

Case Study	Landslide Type	Activation Dates (Calibration + Validation)	t_b (Days)	Φ_c (Calibration)	Φ_v (Validation)
Acri—Serra di Buda	rock slide	5 + 1	74	82.8%	62.2%
San Benedetto Ullano—San Rocco	rock slide	2 + 1	46	100%	96.2%
San Fili—Uncino	rock slide	5 + 1	66	100%	100%
Sorrento Peninsula	soil slip	10 + 1	28	80.6%	76.3%

The base times of the optimal kernels for the considered case studies are quite consistent with landslide magnitudes, being t_b of the Sorrento Peninsula about a half of the Calabrian cases. Base times also reflect permeability and extent of underground water patterns of the drainage basins feeding the landslide sites. In the case of the shallow landslides of the Sorrento Peninsula, shorter base times and higher influence of most recent rainfall can be observed with respect to the Calabrian rock slides, evidencing a faster slope stability response to rainfall as potential triggering factor.

As for the case studies considered in this paper, calibration and validation results show fitness values ranging from 81% to 100 % and from 62% to 100%, respectively. The best model performances were obtained for the case studies of San Fili—Uncino and San Benedetto Ullano—San Rocco, while less satisfactorily results characterize the Sorrento Peninsula and Acri—Serra di Buda cases. It should be noticed that, for the San Rocco landslide, the fitness obtained in validation is affected by a false alarm predicted by the model just the day before the activation of the phenomenon (as known from local archives).

Generally speaking, case studies characterized by fewer activation dates are simpler to model. On the other hand, model performances are known to be hampered by quality or completeness of input data (e.g., missing dates of activation; dates related to other triggering factors; unsuitability of the rain gauge network) [65]. Furthermore, available rain gauges are usually far from the sites of interest, and located at either different elevations or aspects. Uncertainty in rainfall estimation has a strong impact on the identification of the triggering rainfall [66,67]. Still, information regarding activation dates is commonly incomplete or poorly accurate [10]. As a whole, such uncertainties may strongly affect the calibration and the validation of the models.

In this study, the best results obtained were presumably favored by:

- accurate recording of damaging events along the railway track, for the Uncino rock slide;
- accurate monitoring of landslide activations and damaging events at the margin of the village, for the San Rocco rock slide;
- good representativeness of the rainfall series recorded at the Montalto Uffugo rain gauge, for both the Uncino and the San Rocco rock slides.

As for the weakest results, they may be explained by considering the following issues:

- for the Sorrento Peninsula case study, significant heterogeneities in slope materials and differences in extent of shallow landslides reasonably affected model performances. In addition, dates of landslide activation may be missing, especially for soils slips triggered in remote areas. Rainfall events responsible for shallow landslide activations are usually short and spatially limited (e.g., convective storms), and can barely be recorded by the rain gauge network. Consequently, the representativeness of the rain series cannot be guaranteed for such type of meteoric events.

- for the Acri case study, some of the considered activations may refer to secondary portions of the rock slide. For some dates, historical archives are not, in fact, detailed enough to permit an accurate understanding of the mobilized volumes. Consequently, movements affecting only portions of the rock slide—or even other nearby landslides developed in the same Sackung—may be erroneously attributed to the investigated phenomenon.

5. Conclusions and Perspectives

In the present paper, examples of application of $^{GA}SAKe$ have been presented, with reference to soil slips and rock slides in Southern Italy. For all cases, both calibration and validation of the model were performed using independent datasets. Obtained results sound either excellent (cf. San Fili—Uncino and San Benedetto Ullano—San Rocco cases) or just promising (Sorrento Peninsula, and Acri—Serra di Buda cases).

For the Uncino and the San Rocco landslides, the activation dates are correctly predicted by the model, evidently thanks to an accurate knowledge of the activation history of the landslide, and a proper hydrological characterization of the site. For such case, $^{GA}SAKe$ could be applied to predict the timing of activation of future landslide activations in the same areas. Thanks to kernels obtained in calibration, the model could be usefully employed within early-warning systems for geo-hydrological risk mitigation and Civil Protection purposes, also based on predicted rainfall.

Conversely, for the Serra di Buda and the Sorrento Peninsula cases, weaker model performances appear to be influenced by an inaccurate knowledge of the activation dates and/or rainfall series—as generally occurs with hydrological models. Nevertheless, such results still sound encouraging, provided that quality and completeness of data were improved. For past activations, further investigations may allow to better define the history of landslide mobilizations in the considered areas; rainfall data recorded at the surface by the gauge network may profitably be combined with weather radar prospectings (cf. e.g., [68,69]). Moreover, it would be desirable that regional geological and hydrographic services were strengthened to guarantee adequate activities of surveying and monitoring of the geo-hydrological events, by implementing and updating suitable data bases on triggered slope movements (including details such as location, type, type of involved materials, dates of activation, damage). As for the rains, the networks may be improved by adding further gauges and/or radar installations.

It is worth observing that, due to its empirical/hydrological nature, $^{GA}SAKe$ needs a representative sample of data for calibration and validation. Such phases are both crucial for properly tuning any prediction model, particularly when it is aimed at being implemented into an early-warning system. In some of the cases analyzed in this paper, the number of available activation dates was not large enough to permit the selection of different sub-samples, thus only one date of activation (i.e., the last) was considered for all validations. Nevertheless, such type of approach can be viewed in terms of an “operative” application of the model in an operational warning system (i.e., used to predict the “next” activation, based on the known history of landslide movements in a given area).

With respect to other empirical/hydrological models, the main advantages implemented in $^{GA}SAKe$ are: (i) the automatic calibration of the model by means of genetic algorithms; (ii) the high degrees of freedom of the kernel (in fact, a fixed mathematical function is not required). The adoption of Genetic Algorithms allows for a thorough exploration of the “solution space”, and guarantees that best solutions to any problem can be obtained (following Holland’s Fundamental Theorem [24]). Moreover, the initial shape of the kernel can be suggested from the operator or even left at random. During model iterations, the shape of the kernels evolves (as their length), thanks to genetic operators, and can reach any type of final configuration. The above features are deemed of outmost value, as they allow to limit subjectivity in the application of a model [70].

If analyzed in detail, the kernels obtained with $^{GA}SAKe$ may appear difficult to understand in physical terms. Nevertheless, in most real cases, slope instability needs to be explained by a complex interplay of several groundwater paths. These latter commonly result in kernels with

quite irregular patterns, and cannot be simulated by simplified analytical functions. According to [71], kernels characterized by complex patterns (and many parameters) are commonly needed to simulate groundwater dynamics. Being characterized by higher complexity, resulting kernels do not necessarily imply greater predictive uncertainties [72,73].

A new release of the model is presently being tested against a set of case studies of different types and extent, selected in diverse geological contexts. Among the improvements, some concern the Genetic Algorithms utilized for the optimization: in particular, a set of selection criteria (roulette, ranking, stochastic tournament, deterministic tournament) will be available shortly, also considering different combinations of ordering criteria (by including the safety margin, the base time, and the first-order momentum to the main fitness of the kernel). Obtained kernels can be post-processed and analyzed in terms of either control points or analytical functions, to allow for deeper hydro-geological ruminations. The final regression of kernels into analytical functions may allow a better understanding of complex groundwater behaviors, and hence landslide responses to antecedent rainfall. Finally, some computational improvements concern smaller requirements of storage capacity and higher execution speed, thanks to parallel optimization that allows for reducing elaborations by ca. 1/50, which will allow improvements in the model performances for an effective implementation in early-warning systems.

Acknowledgments: Authors are grateful to Alessio De Rango, Donato D’Ambrosio, William Spataro, and Rocco Rongo (Department of Mathematics and Informatics, University of Calabria, Italy) for discussions and support in the development and testing phases of the model. Authors acknowledge the Editor and three anonymous Referees for their comments and suggestions that allowed improvements to the original version of the manuscript.

Author Contributions: All the authors contributed to the design and implementation of the research, to the analysis of the results and to the preparation of the manuscript.

Conflicts of Interest: The authors declare no conflict of interest.

References

1. Guzzetti, F. Landslides fatalities and the evaluation of landslide risk in Italy. *Eng. Geol.* **2000**, *58*, 89–107. [[CrossRef](#)]
2. Iovine, G.; Gariano, S.L.; Terranova, O. Alcune riflessioni sull’esposizione al rischio da frane superficiali alla luce dei recenti eventi in Italia meridionale. *Geologi Calabria* **2009**, *10*, 4–31. (In Italian)
3. Peruccacci, S.; Brunetti, M.T.; Gariano, S.L.; Melillo, M.; Rossi, M.; Guzzetti, F. Rainfall thresholds for possible landslide occurrence in Italy. *Geomorphology* **2017**, *290*, 39–57. [[CrossRef](#)]
4. Greco, R.; Comegna, R.; Damiano, E.; Guida, A.; Olivares, L.; Picarelli, L. Hydrological modelling of a slope covered with shallow pyroclastic deposits from field monitoring data. *Hydrol. Earth Syst. Sci.* **2013**, *17*, 4001–4013. [[CrossRef](#)]
5. Peres, D.J.; Cancelliere, A. Derivation and evaluation of landslide-triggering thresholds by a Monte Carlo approach. *Hydrol. Earth Syst. Sci.* **2014**, *18*, 4913–4931. [[CrossRef](#)]
6. Alvioli, M.; Baum, R.L. Parallelization of the TRIGRS model for rainfall-induced landslides using the message passing interface. *Environ. Modell. Softw.* **2016**, *81*, 122–135. [[CrossRef](#)]
7. Rossi, M.; Peruccacci, S.; Brunetti, M.T.; Marchesini, I.; Luciani, S.; Ardizzone, F.; Balducci, V.; Bianchi, C.; Cardinali, M.; Fiorucci, F.M. SANF: National warning system for rainfall-induced landslides in Italy. In *Landslides and Engineered Slopes: Protecting Society through Improved Understanding*; Taylor & Francis Group: London, UK, 2012; pp. 1895–1899.
8. De Luca, D.; Versace, P. Diversity of rainfall thresholds for early warning of hydro-geological disasters. *Adv. Geosci.* **2017**, *44*, 53–60. [[CrossRef](#)]
9. Vennari, C.; Gariano, S.L.; Antronico, L.; Brunetti, M.T.; Iovine, G.; Peruccacci, S.; Terranova, O.; Guzzetti, F. Rainfall thresholds for shallow landslide occurrence in Calabria, southern Italy. *Nat. Hazards Earth Syst. Sci.* **2014**, *14*, 317–330. [[CrossRef](#)]

10. Gariano, S.L.; Brunetti, M.T.; Iovine, G.; Melillo, M.; Peruccacci, S.; Terranova, O.; Vennari, C.; Guzzetti, F. Calibration and validation of rainfall thresholds for shallow landslide forecasting in Sicily, southern Italy. *Geomorphology* **2015**, *228*, 653–665. [[CrossRef](#)]
11. Pisano, L.; Vennari, C.; Vessia, G.; Trabace, M.; Amoroso, G.; Loiacono, P.; Parise, M. Data collection for reconstructing empirical rainfall thresholds for shallow landslides: Challenges and improvements in the Daunia Sub-Apennine (Southern Italy). *Rend. Online Soc. Geol. Ital.* **2015**, *35*, 236–239. [[CrossRef](#)]
12. Melillo, M.; Brunetti, M.T.; Peruccacci, S.; Gariano, S.L.; Guzzetti, F. Rainfall thresholds for the possible landslide occurrence in Sicily (Southern Italy) based on the automatic reconstruction of rainfall events. *Landslides* **2016**, *13*, 165–172. [[CrossRef](#)]
13. Piciullo, L.; Gariano, S.L.; Melillo, M.; Brunetti, M.T.; Peruccacci, S.; Guzzetti, F.; Calvello, M. Definition and performance of a threshold-based regional early warning model for rainfall-induced landslides. *Landslides* **2017**, *14*, 995–1008. [[CrossRef](#)]
14. Iovine, G.; Iaquina, P.; Terranova, O. Emergency management of landslide risk during Autumn-Winter 2008/2009 in Calabria (Italy). The example of San Benedetto Ullano. In Proceedings of the 18th World IMACS Congress and MODSIM09 International Congress on Modelling and Simulation, Cairns, Australia, 13–17 July 2009; pp. 2686–2693.
15. Iovine, G.; Petrucci, O.; Rizzo, V.; Tansi, C. The March 7th 2005 Cavallerizzo (Cerzeto) landslide in Calabria-Southern Italy. In Proceeding of the 10th IAEG Congress: Engineering Geology for Tomorrow's Cities, Nottingham, UK, 6–10 September 2006.
16. Terranova, O.; Lollino, P.; Gariano, S.L.; Iaquina, P.; Iovine, G. Un sistema integrato di sorveglianza per la mitigazione del rischio da frana. *Geologi Calabria* **2010**, *11*, 6–28. (In Italian)
17. Terranova, O.; Gariano, S.L.; Iaquina, P.; Iovine, G. ^{GA}SAKe: Forecasting landslide activations by a genetic-algorithms-based hydrological model. *Geosci. Model Dev.* **2015**, *8*, 1955–1978. [[CrossRef](#)]
18. Terranova, O.; Iaquina, P.; Gariano, S.L.; Greco, R.; Iovine, G. ^{CM}SAKe: A hydrological model to forecasting landslide activations. In *Landslide Science and Practice*; Springer: Berlin, Germany, 2013; pp. 73–79.
19. Sirangelo, B.; Versace, P. A real time forecasting for landslides triggered by rainfall. *Meccanica* **1996**, *31*, 1–13. [[CrossRef](#)]
20. Capparelli, G.; Versace, P. FLaiR and SUSHI: Two mathematical models for early warning of landslides induced by rainfall. *Landslides* **2011**, *8*, 67–79. [[CrossRef](#)]
21. Peres, D.J.; Cancelliere, A. Defining rainfall thresholds for early warning of rainfall-triggered landslides: The case of North-East Sicily. In *Landslide Science and Practice*; Springer: Berlin, Germany, 2013; pp. 257–263.
22. Capparelli, G.; Giorgio, M.; Greco, R. Shallow landslides risk mitigation by early warning: The Sarno case. In *Landslide Science and Practice*; Springer: Berlin, Germany, 2013; pp. 767–772.
23. Greco, R.; Giorgio, M.; Capparelli, G.; Versace, P. Early warning of rainfall-induced landslides based on empirical mobility function predictor. *Eng. Geol.* **2013**, *153*, 68–79. [[CrossRef](#)]
24. Holland, J.H. *Adaptation in Natural and Artificial Systems: An Introductory Analysis with Applications to Biology, Control and Artificial Intelligence*; MIT Press: Cambridge, MA, USA, 1992; ISBN 0262082136.
25. D'Ambrosio, D.; Spataro, W.; Rongo, R.; Iovine, G. Genetic algorithms, optimization, and evolutionary modeling. In *Treatise on Geomorphology. Quantitative Modeling of Geomorphology*; Shroder, J., Baas, A.C.W., Eds.; Academic Press: San Diego, CA, USA, 2013; pp. 74–97.
26. Amodio-Morelli, L.; Bonardi, G.; Colonna, V.; Dietrich, D.; Giunta, G.; Ippolito, F.; Liguori, V.; Lorenzoni, S.; Paglionico, A.; Perrone, V. L'arco calabro-peloritano nell'orogene appenninico-maghrebide. *Mem. Soc. Geol. Ital.* **1976**, *17*, 1–60. (In Italian)
27. Monaco, C.; Tortorici, L. Active faulting in the Calabrian Arc and eastern Sicily. *J. Geodyn.* **2000**, *29*, 407–424. [[CrossRef](#)]
28. Tortorici, L.; Monaco, C.; Tansi, C.; Cocina, O. Recent and active tectonics in the Calabrian Arc (southern Italy). *Tectonophysics* **1995**, *243*, 37–55. [[CrossRef](#)]
29. Van Dijk, J.P.; Bello, M.; Brancaleoni, G.P.; Cantarella, G.; Costa, V.; Frixia, A.; Golfetto, F.; Merlini, S.; Riva, M.; Torricelli, S.; Toscano, C.; Zerilli, A. A regional structural model for the northern sector of the Calabrian Arc (southern Italy). *Tectonophysics* **2000**, *324*, 267–320. [[CrossRef](#)]
30. Tansi, C.; Muto, F.; Critelli, S.; Iovine, G. Neogene-Quaternary strike-slip tectonics in the central Calabrian Arc (southern Italy). *J. Geodyn.* **2007**, *43*, 393–414. [[CrossRef](#)]

31. Sorriso-Valvo, G.M. Mass movements and slope evolution in Calabria. Proceedings of 4th International Conference and Field Workshop on Landslides, Tokyo, Japan, 23–31 August 1985; pp. 23–30.
32. Carrara, A.; Catalano, E.; Sorriso-Valvo, G.M.; Reali, C.; Merenda, L.; Rizzo, V. Landslide morphometry and typology in two zones, Calabria, Italy. *Bull. Eng. Geol. Environ.* **1977**, *16*, 8–13.
33. Carrara, A.; Merenda, L.; Nicoletti, P.G.; Sorriso-Valvo, G.M. Slope instability in Calabria, Italy. In Proceedings of the Polish-Italian Seminar on Superficial Mass Movement in Mountain Regions, Szymbark, Poland, 17–19 May 1979; pp. 47–62.
34. Crescenzi, E.; Grassi, D.; Iovine, G.; Merenda, L.; Miceli, F.; Sdao, F. Fenomeni di instabilità franosa nei centri abitati calabresi: Esempi rappresentativi. *Geol. Appl. Hydrogeol.* **1996**, *31*, 203–226. (In Italian)
35. Iovine, G.; Merenda, L. Nota illustrativa alla “Carta delle frane e della mobilitazione diastrofica dal 1973 ad oggi nel bacino del Torrente Straface (Alto Jonio; Calabria)”. *Geol. Appl. Hydrogeol.* **1996**, *31*, 107–128. (In Italian)
36. Iovine, G.; Petrucci, O. Effetti sui versanti e nel fondovalle indotti da un evento pluviale eccezionale nel bacino di una fiumara calabrese (T. Pagliara). *Boll. Soc. Geol. Ital.* **1998**, *117*, 821–840. (In Italian)
37. Iovine, G.; Parise, M.; Tansi, C. Slope movements and tectonics in North-Eastern Calabria (Southern Italy). In Proceedings of the 7th International Symposium on Landslides (ISL’96): Landslides Glissements de Terrain, Trondheim, 17–21 June 1996; pp. 785–790.
38. Ferrari, E.; Iovine, G.; Petrucci, O. Evaluating landslide hazard through geomorphologic, hydrologic and historical analyses in north-eastern Calabria (southern Italy). In Proceedings of the EGS Plinius Conference on Mediterranean Storms, Maratea, Italia, 14–16 October 1999; pp. 425–438.
39. Tansi, C.; Iovine, G.; Folino-Gallo, M. Tettonica attiva e recente; e manifestazioni gravitative profonde; lungo il bordo orientale del graben del Fiume Crati (Calabria settentrionale). *Boll. Soc. Geol. Ital.* **2005**, *124*, 563–578. (In Italian)
40. Köppen, W.P. *Climatologia con un Estudio de los Climas de la Tierra*; Fondo de Cultura Economica: Ciudad de Mexico City, Mexico, 1948; p. 479.
41. Terranova, O. Caratteristiche degli eventi pluviometrici a scala giornaliera in Calabria. In Proceeding of the XXIX Convegno di Idraulica e Costruzioni Idrauliche, Trento, Italy, 7–10 September 2004; pp. 343–350. (In Italian)
42. Terranova, O.; Gariano, S.L. Rainstorms able to induce flash floods in a Mediterranean-climate region (Calabria, southern Italy). *Nat. Hazard Earth Syst. Sci.* **2014**, *14*, 2423–2434. [[CrossRef](#)]
43. Ferrari, E.; Terranova, O. Non-parametric detection of trends and change point years in monthly and annual rainfalls. In Proceedings of the 1st Italian-Russian Workshop on New Trend in Hydrology, Rende (CS), Italy, 24–26 September 2002; pp. 177–188. (In Italian)
44. Terranova, O.; Gariano, S.L. Regional investigation on seasonality of erosivity in the Mediterranean environment. *Environ. Earth Sci.* **2015**, *73*, 311–324. [[CrossRef](#)]
45. Iovine, G.; Tansi, C.; Folino-Gallo, M. Strutture da accomodamento tettono-gravitativo nell’evoluzione tardiva dei sistemi di catena: Il caso di studio di Acri (Calabria settentrionale). *Boll. Soc. Geol. Ital.* **2004**, *123*, 39–51. (In Italian)
46. Tansi, C.; Talarico, A.; Iovine, G.; Folino Gallo, M.; Falcone, G. Interpretation of radon anomalies in seismotectonic and tectonic-gravitational setting of the south-eastern Crati Graben (Northern Calabria, Italy). *Tectonophysics* **2005**, *396*, 181–193. [[CrossRef](#)]
47. *Carta Geologica della Calabria*; CASMEZ: Ercolano, Napoli, Italia, 1967. (In Italian)
48. Sorriso-Valvo, G.M. *1:250,000 Scale Map of the Large Landslides and of the Deep-Seated Gravitational Slope Deformations of Calabria*; Selca: Firenze, Italia, 1996.
49. Terranova, O.; Antronico, L.; Gullà, G. Landslide triggering scenarios in homogeneous geological contexts: The area surrounding Acri (Calabria, Italy). *Geomorphology* **2007**, *87*, 250–267. [[CrossRef](#)]
50. Gariano, S.L.; Terranova, O.G.; Greco, R.; Iaquina, P.; Iovine, G. Forecasting the timing of activation of rainfall-induced landslides. An application of GA-SAKE to the Acri case study (Calabria, Southern Italy). *Geophys. Res. Abstr.* **2013**, *15*, EGU2013-678.
51. Iovine, G.; Lollino, P.; Gariano, S.L.; Terranova, O. Coupling limit equilibrium analyses and real-time monitoring to refine a landslide surveillance system in Calabria (southern Italy). *Nat. Hazard Earth Syst. Sci.* **2010**, *10*, 2341–2354. [[CrossRef](#)]

52. Capparelli, G.; Iaquina, P.; Iovine, G.; Terranova, O.G.; Versace, P. Modelling the rainfall-induced mobilization of a large slope movement in northern Calabria. *Nat. Hazards* **2012**, *61*, 247–256. [[CrossRef](#)]
53. Sorriso-Valvo, G.M.; Antronico, L.; Catalano, E.; Gullà, G.; Tansi, C.; Dramis, F.; Ferrucci, F.; Fantucci, R. *The Temporal Stability and Activity of Landslides in Europe with Respect to Climatic Change (TESLEC)*; Final Report; Istituto di Ricerca per la Protezione Idrogeologica (IRPI): Turin, Italy, 1996.
54. Iovine, G.; De Rango, A.; Gariano, S.L.; Terranova, O. Forecasting landslide activations by means of GA-SAKE. An example of application to three case studies in Calabria (Southern Italy). *Geophys. Res. Abstr.* **2016**, *18*, 4645.
55. Ippolito, F.; D'Argenio, B.; Pescatore, T.; Scandone, P. Structural–stratigraphic units and tectonic framework of Southern Apennines. In *Geology of Italy*; Squyres, C., Ed.; Earth Sciences Society of the Libyan Arab Republic: Tripoli, Libya, 1975; pp. 317–328.
56. Di Crescenzo, G.; Santo, A. Analisi morfologica delle frane da scorrimento-colata rapida in depositi piroclastici della Penisola Sorrentina (Campania). *Geogr. Fis. Dinam. Quat.* **1999**, *22*, 57–72. (In Italian)
57. Ducci, D.; Tranfaglia, G. L'impatto dei cambiamenti climatici sulle risorse idriche sotterranee in Campania. *Boll. Ordine Geol. Campania* **2005**, *1–4*, 13–21. (In Italian)
58. Servizio Idrografico. *Annali Idrologici: Parte I*; Compartimento di Napoli, Istituto poligrafico e Zecca dello Stato: Rome, Italy, 1948–1999.
59. Rossi, F.; Villani, P. *Valutazione Delle Piene in Campania*; CNR-GNDICI publications No. 1470; Grafica Metelliana: Cava de' Tirreni, Italia, 1994. (In Italian)
60. Mele, R.; Del Prete, S. Lo studio della franosità storica come utile strumento per la valutazione della pericolosità da frane. Un esempio nell'area di Gragnano (Campania). *Boll. Soc. Geol. Ital.* **1999**, *118*, 91–111. (In Italian)
61. Calcaterra, D.; Santo, A. The January 10, 1997 Pozzano landslide, Sorrento Peninsula, Italy. *Eng. Geol.* **2004**, *75*, 181–200.
62. Di Crescenzo, G.; Santo, A. Debris slides-rapid earth flows in the carbonate massifs of the Campania region (Southern Italy): Morphological and morphometric data for evaluating triggering susceptibility. *Geomorphology* **2005**, *66*, 255–276.
63. Cascini, L.; Sorbino, G.; Cuomo, S.; Ferlisi, S. Seasonal effects of rainfall on the shallow pyroclastic deposits of the Campania region (southern Italy). *Landslides* **2014**, *11*, 779–792. [[CrossRef](#)]
64. Terranova, O.; Greco, V.R.; Gariano, S.L.; Pascale, S.; Rago, V.; Caloiero, P.; Iovine, G. Monitoring and modelling for landslide risk mitigation and reduction. The case study of San Benedetto Ullano (Northern Calabria-Italy). *Geophys. Res. Abstr.* **2016**, *18*, 4708.
65. Peres, D.J.; Cancelliere, A.; Greco, R.; Bogaard, T.A. Influence of uncertain identification of triggering rainfall on the assessment of landslide early warning thresholds. *Nat. Hazards Earth Syst. Sci. Discuss.* **2017**. [[CrossRef](#)]
66. Nikolopoulos, E.I.; Crema, S.; Marchi, L.; Marra, F.; Guzzetti, F.; Borga, M. Impact of uncertainty in rainfall estimation on the identification of rainfall thresholds for debris flow occurrence. *Geomorphology* **2014**, *221*, 286–297. [[CrossRef](#)]
67. Marra, F.; Destro, E.; Nikolopoulos, E.I.; Zoccatelli, D.; Creutin, J.D.; Guzzetti, F.; Borga, M. Impact of rainfall spatial aggregation on the identification of debris flow occurrence thresholds. *Hydrol. Earth Syst. Sci.* **2017**, *21*, 4525–4532. [[CrossRef](#)]
68. Gabriele, S.; Terranova, O.; Pascale, S.; Rago, V.; Chiaravalloti, F.; Sabatino, P.; Brocca, L.; Laviola, S.; Baldini, L.; Federico, S. RAMSES: A nowcasting system for mitigating geo-hydrological risk along the railway. *Geophys. Res. Abstr.* **2016**, *18*, 8462.
69. Rago, V.; Chiaravalloti, F.; Chiodo, G.; Gabriele, S.; Lupiano, V.; Nicastro, R.; Pellegrino, A.D.; Procopio, A.; Siviglia, S.; Terranova, O.G.; Iovine, G. Geomorphic effects caused by heavy rainfall in southern Calabria (Italy) on 30 October–1 November 2015. *J. Maps* **2017**, *13*, 836–843. [[CrossRef](#)]
70. D'Ambrosio, D.; Spataro, W.; Rongo, R.; Iovine, G. Genetic algorithms, optimization, and evolutionary modeling. In *Treatise on Geomorphology, Volume 2, Quantitative Modeling of Geomorphology*; Baas, A., Ed.; Academic Press: San Diego, CA, USA, 2013; pp. 74–97.
71. Pinault, J.-L.; Plagnes, V.; Aquilina, L. Inverse modeling of the hydrological and the hydrochemical behavior of hydrosystems: Characterization of karst system functioning. *Water Resour. Res.* **2001**, *37*, 2191–2204. [[CrossRef](#)]

72. Fielen, M.N.; Doherty, J.E.; Hunt, R.J.; Reeves, H. *Using Prediction Uncertainty Analysis to Design Hydrologic Monitoring Networks: Example Applications from the Great Lakes Water Availability Pilot Project*; Scientific Investigations Report 2010-5159, U.S. Geological Survey: Reston, VA, USA, 2010.
73. Long, A.J. RRAWFLOW: Rainfall-response aquifer and watershed flow model (v1.15). *Geosci. Model Dev.* **2015**, *8*, 865–880. [[CrossRef](#)]



© 2018 by the authors. Licensee MDPI, Basel, Switzerland. This article is an open access article distributed under the terms and conditions of the Creative Commons Attribution (CC BY) license (<http://creativecommons.org/licenses/by/4.0/>).